Climate Applications from High Spectral Resolution Infrared Sounders

Mitchell D. Goldberg, Lihang Zhou , and Xingpin Liu

National Oceanic and Atmospheric Administration, National Environmental Satellite, Data, and Information Service, Center for Satellite Applications and Research
Camp Springs, Maryland, USA.

Abstract

There is growing consensus that persistent and increasing anthropogenic emissions, since the beginning of the industrial revolution in the 19th century, are increasing atmospheric temperatures, increasing sea levels, melting ice caps and glaciers, increasing the occurrence of severe weather, and causing regional shifts in precipitation patterns. Changes in these parameters or occurrences are responses to changes in climate forcing terms, notably greenhouse gases. The NASA Atmospheric InfraRed Sounder (AIRS) [Aumann et al., 2003], launched in May of 2002, is the first high spectral resolution infrared sounder with nearly complete global coverage on a daily basis. High spectral resolution in the infrared provides sensitivity to nearly all climate forcings, responses and feedbacks. The AIRS radiances are sensitive to changes in carbon dioxide, methane, carbon monoxide, ozone, water vapor, temperature, clouds, aerosols, and surface characteristics. The AIRS data are applied to generate the first ever spectrally resolved infrared radiance (SRIR) dataset (2002- 2006) for monitoring changes in atmospheric temperature and constituents and for assessing the accuracy of climate and weather model analyses and forecasts [Goldberg, 2009]. The SRIR dataset is a very powerful climate application. Spectral signatures derived from the dataset confirmed the largest depletion of ozone over the Arctic in 2005, and also verified that the European Center for Medium Range Weather (ECMWF) model analysis water vapor fields are significantly more accurate than the analyses of the National Centers for Environmental Prediction (NCEP). The NCEP moisture fields are generally 20% more moist than those from ECMWF. Applications included computations of radiances from NCEP and ECMWF atmospheric states and comparison of these calculated radiances with those obtained from the SRIR dataset. Comparisons showed very good agreement between the SRIR data and ECMWF simulated radiances, while the agreement with NCEP values was rather poor. However, further comparisons with the SRIR dataset in 2006 found degradation in the ECMWF upper tropospheric water vapor fields due to an operational change in ECMWF assimilation /modeling procedures. This unexpected result demonstrates the importance of continuous routine monitoring. The SRIR climatology will be extended into the future using AIRS and the EUMETSAT Infrared Atmospheric Interferometer Sounder (IASI) and the NPOESS Cross-track Infrared Sounder (CrIS). The current SRIR dataset will be extended to 2009 by the end of 2010.

Obviously there are numerous other climate applications, such as using derived retrievals of the atmospheric state (including trace gases) to monitor climate change and to validate other datasets. However, since retrievals are based on algorithms which vary based on the developers. The results would be questionable, since two different retrievals often produce different results. More intercomparisons of different retrieval techniques would be needed to estimate the uncertainty. Here we limit our climate application to the direct use of radiances, which particularly for AIRS and IASI are much more certain.

1. Introduction

Key factors in generating climate quality products from high spectral resolution infrared sounders are adequate spectral resolution and coverage, excellent signal to noise performance and long term stability. AIRS and IASI have been successful in meeting those factors. The radiometric accuracy and stability of AIRS and IASI radiances have been confirmed by several fundamentally different types of comparisons, including the results of the daily measurements of sea surface temperature (SST) [Aumman et al., 2006], direct spectral radiance comparisons from aircraft observations [Tobin et al., 2006]; and more recently direct intercoomparisons between IASI and AIRS, which have shown that both AIRS and IASI are extremely stable and accurate. The differences between both AIRS and IASI are approximately 0.1 K with a projected stability of 0.1 K per decade [Tobin et al., 2008], [Wang et al, 2009ab]. Fig. 1 shows the AIRS spectral coverage and gaseous absorption

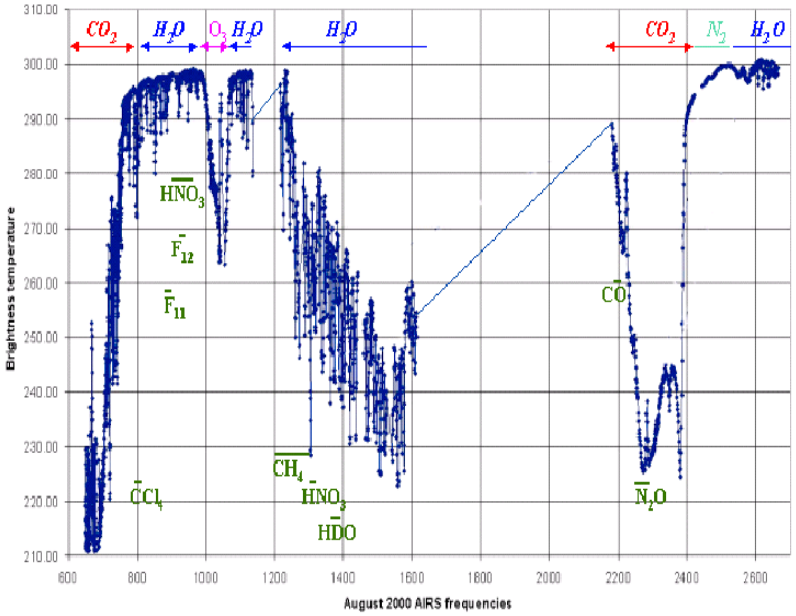

Figure 1: Measured AIRS infrared spectrum contains a wealth of information on the atmosphere including water vapor, temperature and trace gases constituents such as CO2, CO, CH4, O3 and SO2

The SRIR datasets will allow the generation of difference fields for various time periods and regions. Fig. 2 shows the expected change in radiances due to changes in the state field. For example, in this figure one can see that a 15% increase in ozone results in a brightness temperature reduction of approximately 2 K, and a 15% increase in water vapor causes a reduction of approximately 1.25 K

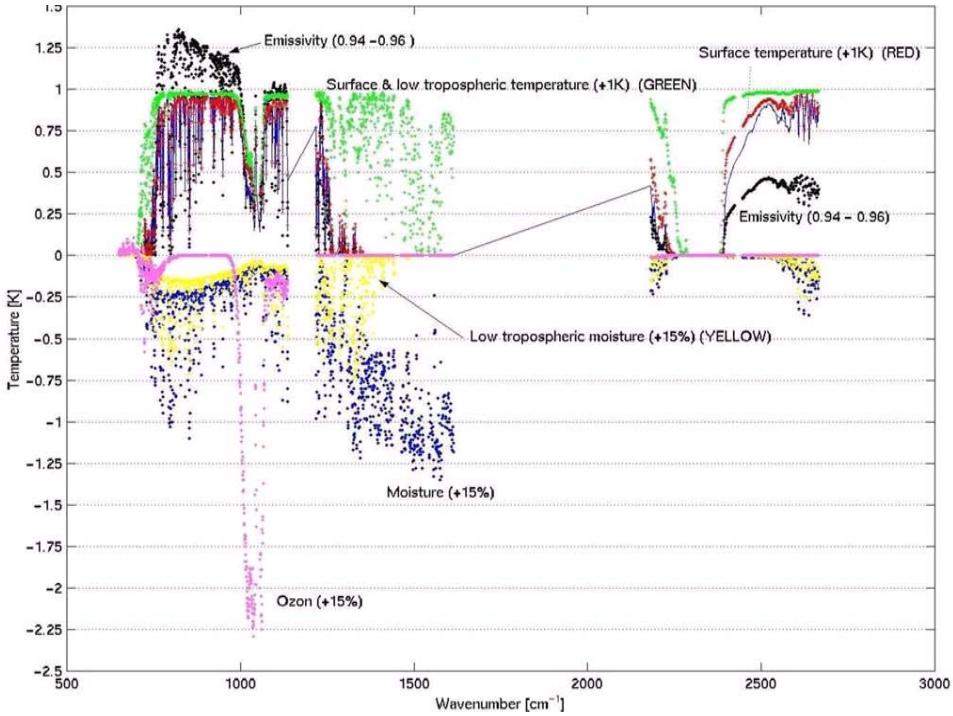

Figure 2: Response in brightness temperatures due to a change in atmospheric and surface parameters

2. Methodology

The SRIR datasets are generated by the following steps: 1) The AIRS observations are screened for outliers, 2) the observations are converted to brightness temperatures and mapped into ascending and descending daily brightness temperature (BT) gridded datasets, 3) the observations within the gridded datasets are converted to principal component scores [Goldberg et al, 2003] and stored in principal component (PC) gridded datasets, 4) the PC grids are adjusted for viewing angle (limb darkening) and stored in angle adjusted PC (AAPC) gridded datasets, 5) angle adjusted brightness temperatures are computed from the AAPC datasets and stored in the angle adjusted brightness temperature (AABT) gridded datasets and 6) the BT and AABT daily datasets are screened for clear sky values and averaged to produce monthly clear sky and all sky datasets.

Each daily grid box contains only the first AIRS field of view (all channels) to observe that box that day for ascending and descending orbits

The SRIR climatology consists of monthly brightness temperature datasets of two types – at the original viewing angle and adjusted for viewing angle to a nadir view - for the period 2003 – 2006 for:

1. Ascending (day), clear sky
2. Ascending, all sky
3. Descending (night), clear sky
4. Descending, all sky datasets

The spatial resolution is 2.0 degree latitude by 0.5 degree longitude. The monthly averaging of the original viewing angle is only for diagnostic purposes.

In a separate process, geophysical parameters from the NCEP and ECMWF atmospheric model analyses are interpolated to the same AIRS gridpoints inserted into SARTA to simulate daily clear sky brightness temperature grids. The simulated datasets are used to demonstrate how the SRIR datasets can be applied to the validation of weather and climate models.

The AIRS limb adjustment methodology is based on the AMSU approach [Goldberg et al., 2001] with the exception that the limb adjustment is performed by principal component analysis. Specifically, the first 200 principal component scores are limb adjusted and then the limb adjusted radiances are reconstructed from the limb adjusted principal component score. The predictors for limb adjusting a given principal component score for an off-nadir position to a nadir value is the given principal component score plus the first six principal component scores. Linear regression is used to generate the predictor coefficients. The left panel of Fig. 3 shows an image of the original AIRS radiances and the limb adjusted radiances for an ozone channel. Note the limb effect in the lower image. On the right panel of Fig. 3, we show the monthly averaged field. Again the lower image is the original data without any limb adjustment. Note the signal is not nearly as intense as the upper image, because we did not account for the limb effect.

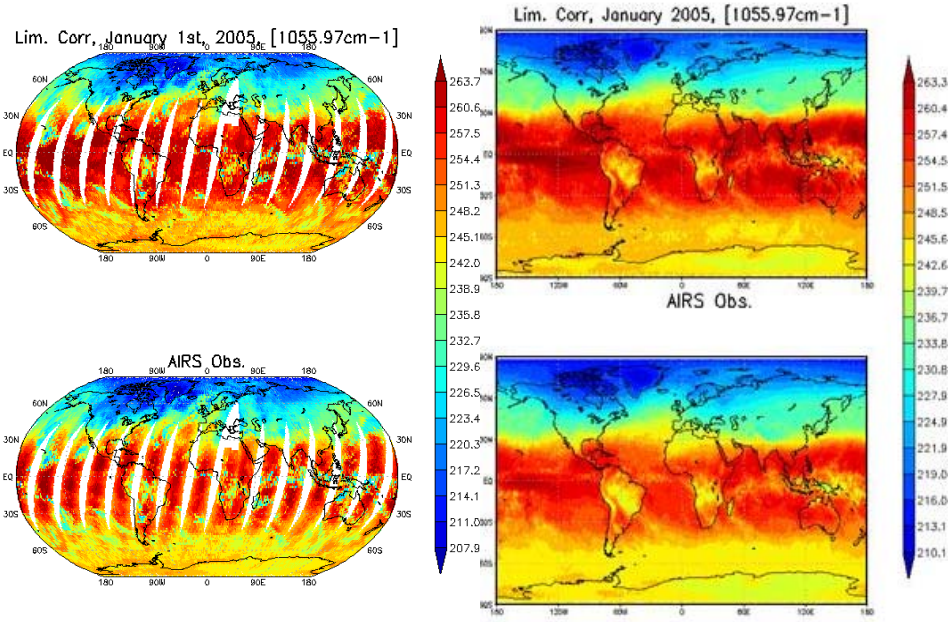

Figure 3: Limb corrected (upper left) and original observed (lower left) AIRS radiance; monthly averaged limb corrected (upper right) and original (lower right) AIRS radiance.

3. Climate Change Detection

The SRIR climatology provides very accurate information on the top of the atmosphere infrared radiance at high spectral resolution. The spectral range is from 650 to 2750 cm^{-1} wavenumbers, equivalent to 15.6 to 3.75 micron wavelengths. Fig. 4 is an example of images which can be produced for an upper tropospheric water vapor channel at 1520.87 cm^{-1}. This figure shows the mean clear-sky brightness temperature for January and July 2005, separated into ascending and descending data (day and night). The patterns are different between July and January. The regions with higher brightness temperatures are generally areas with lower water vapor (due to descending air from Hadley circulation) In these areas, the water vapor weighting functions will peak lower in the atmosphere resulting in warmer brightness temperatures**.**

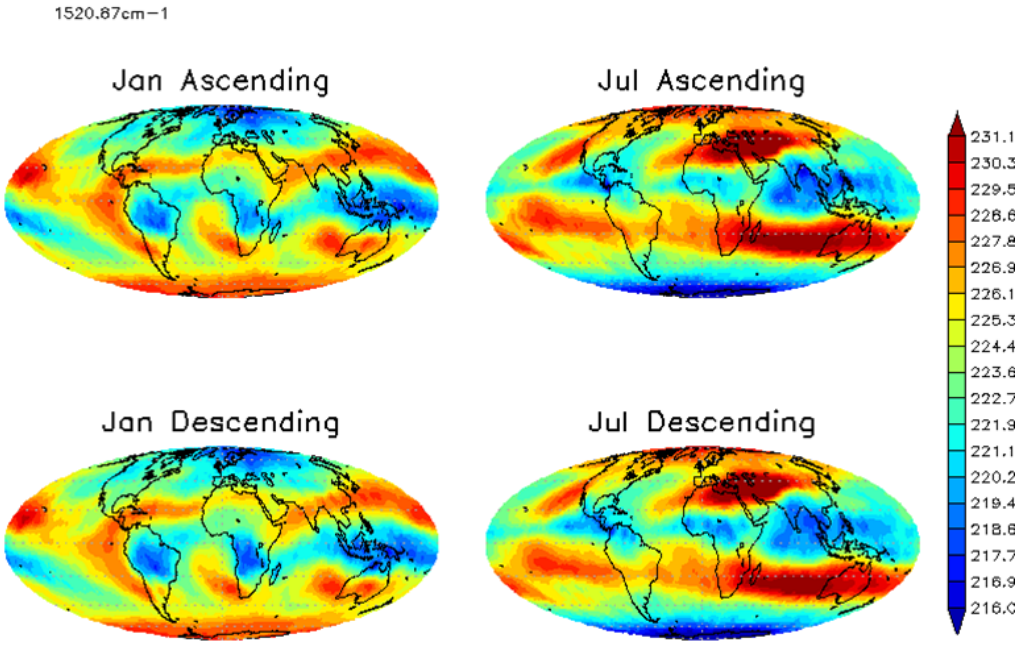

Figure 4: Mean brightness temperature field for January and July 2005 for AIRS water vapor channel centered at 1520.87 cm^{-1}.

Quantitative analysis of differences between different years of spectra can be an indicator of regions experiencing large changes. Since the radiance climatology still covers a relatively short period of time, a search for significant differences was performed by comparing mean spectra from the same month for different years. Fig. 5 shows differences of spectra for July 2004, 2005 and 2006, for all sky conditions (clear, partial clouds, overcast) and for ascending data (day time). (Results for night time are nearly identical) In this example the differences are rather small and spectrally featureless, with the exception of the spectral range of 650 to 700 cm^{-1}, which is sensitive to the upper troposphere and stratosphere. The spectral range of 700 to780 cm^{-1} is sensitive to the mid to lower troposphere. The spectral range of 780 to1000 cm^{-1} is primarily sensitive to the surface (with some weak absorption due to water vapor). And the spectral range of 1000 to1100 cm^{-1} is sensitive to ozone, with the peak of the ozone band at 1040 cm^{-1}. The difference between the two curves is the difference between 2005 and 2006, and the difference is nearly zero, with the exception of a few tenths of a degree in the upper troposphere and stratosphere.

Fig. 6 shows differences of spectra for January 2004, 2005 and 2006. In this figure, there are appreciable differences in the lower to mid troposphere and the surface. However the most noticeable feature is the difference between 2005 and 2004 near the center of the ozone band

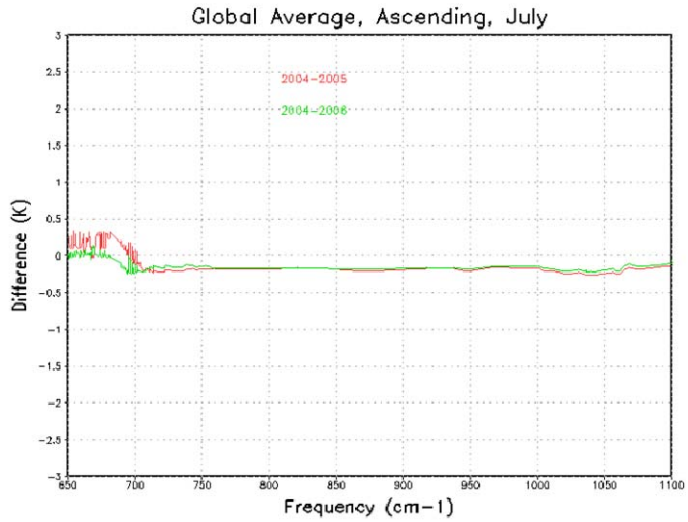

Figure 5: Differences of spectra for July 2004, 2005 and 2006, for all sky conditions (clear, partial clouds, overcast) and for ascending data (day time) between 650 and 1100 cm-1 wavenumber.

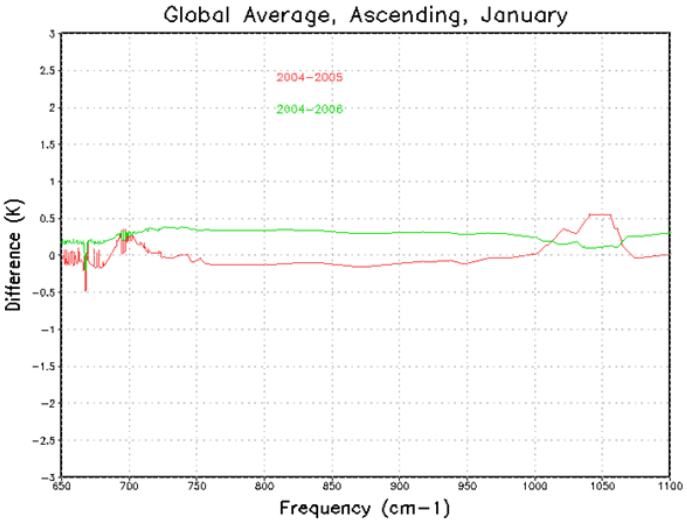

Figure 6: Differences of spectra for January 2004, 2005 and 2006, for all sky conditions (clear, partial clouds, overcast) and for ascending data (day time) between 650 and 1100 cm-1 wavenumber.

In Fig. 7, the global difference fields between 2005 and 2004 show very large departures poleward of 60 degrees north latitude. January 2005, north of Canada, is significantly colder by more than 8 K. An article by *Schiermeier* [2005], Fig. 8, reported on the largest observed depletion in ozone, of approximately 140 Dobsons (relative to a normal amount of 300), in the Arctic in January 2005 as well as very low stratospheric temperatures. The large reduction in the AIRS brightness temperature is due to two factors: a much colder stratosphere as a result of the reduced ozone and the reduced infrared absorption due to the reduced ozone. Theoretically, a 50% change in ozone can cause AIRS brightness temperatures to change by 8 K However, the actual change is dependent on the shape of the temperature profile, since a change in ozone results in the change in the peak and shape of the ozone channel's weighting function. Less ozone broadens the weighting function and reduces its height. So a reduction in ozone results in AIRS observing more of the lower stratosphere. In a nearly isothermal atmosphere, the change in ozone concentration would have very little impact on the brightness temperature, whereas a temperature profile with a large lapse rate will correspond to a significant change in brightness temperature

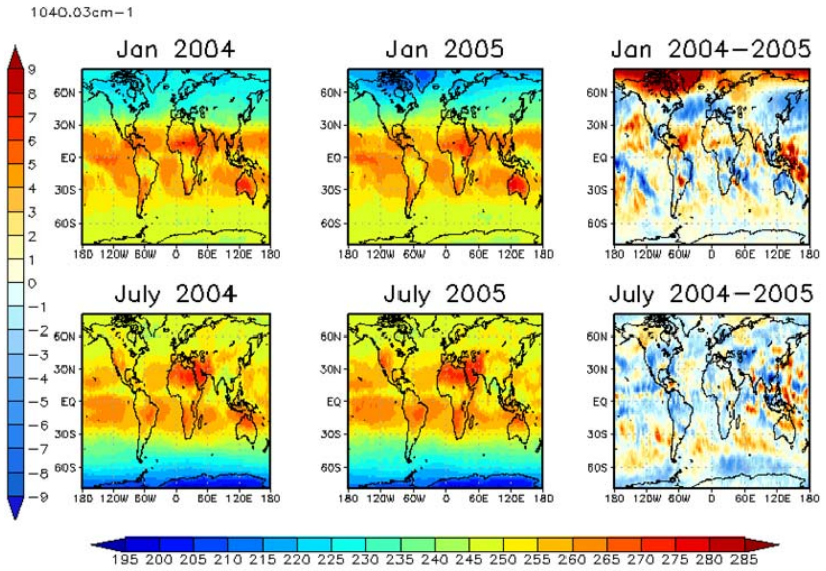

Figure 7: Brightness temperature fields for January, July 2004 and 2005, and their differences for AIRS channel centered at 1040.03 cm-1 wavenumber.

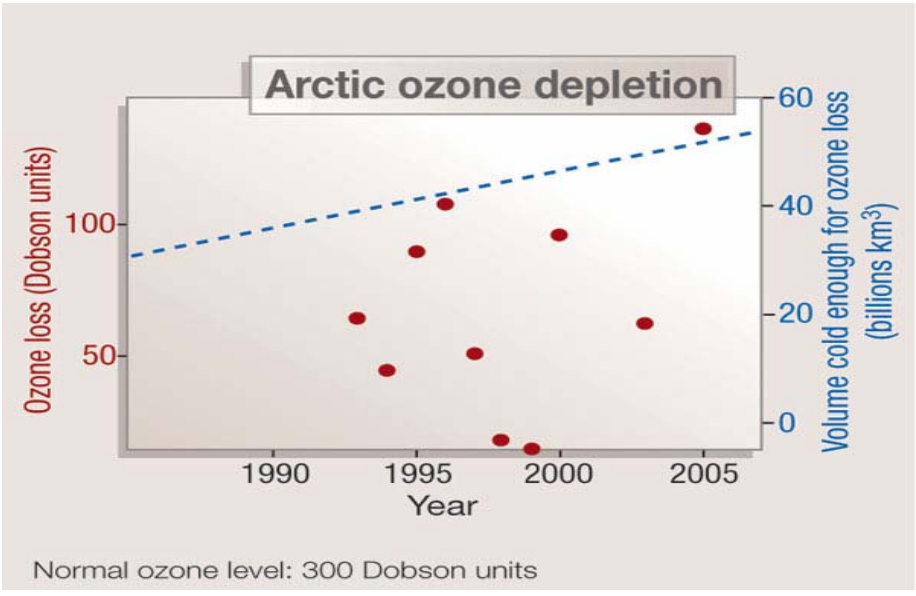

Figure 8: Artic ozone depletion from 1992 to 2005 (from Schiermeier (2005)).

This example shows that the SRIR climatology has significant value for finding and investigating regions of large changes in outgoing longwave radiation at high spectral resolution and then determining which atmospheric constituent contributed to the change.

4. Validation of Model Analyses

The most common analysis methods in NWP are optimum interpolation and variational data assimilation. Both methods make corrections to a first guess forecast (typically a 6 hour forecast from the analysis 6 hours earlier) in such a way that the differences between the corrected first guess and the accepted observations at the analysis time are minimized.

Therefore information from the forecast, which is based on assumptions of model physics, is retained in the analysis. Analysis fields are used to initialize the next series of forecasts and are also used as truth for validating forecasts for different time periods. Analysis fields are used for providing the best estimate of the atmosphere. A climate reanalysis provides a historical collection of analyses from which trends and variability in climate can be assessed. Weather prediction centers, as part of their operations, generate analyses and forecast fields. The fields generated from each center are different due to differing data assimilation and forecast systems. Though the analysis is often regarded as truth, there are different "truths" from different NWP centers. Therefore, it is of utmost importance to independently assess the accuracy of different analysis systems. The use of the SRIR climatology can provide this very important capability.

A very important application of the radiance climatology is to compare model analyses simulated radiances with observed. Generally we found that the ECMWF and NCEP analyses agreed quite well for temperature, with the exception of the upper stratosphere, and for moisture, where NCEP appears to be more moist by 20%. The following figures show the differences in calculated brightness temperatures between NCEP and ECMWF analyses fields for two upper tropospheric temperature channels peaking at 15 and 1.5 mb are shown in Fig. 9. Two two water vapor channels at 1519.07 cm^{-1} (315 mb) and 1598.45 cm^{-1} (490 mb) were selected representing upper and mid tropospheric water vapor, respectfully, and the differences are shown in Fig. 10. The SARTA radiative transfer model [Strow et al., 2003] is used in all calculations.

When compared with measured AIRS brightness temperatures, one can make an assessment of the accuracy of each model. Figure 11 show the differences between limb adjusted AIRS with simulated ECMWF and NCEP brightness temperatures for 667.27 cm^{-1} (15 mb). Figure 12 show the differences for 667.775 cm^{-1} (1.5 mb).

Based on the results given in Figs. 11 and 12, it is clear that the ECMWF temperature analysis is in better agreement with the AIRS radiance climatology. Note the exceptional agreement for the 667.27 cm^{-1} (15 mb) channel. The bias with ECWMF is only about -0.1 K, whereas with NCEP the bias is about - 1 K. In the case of the 667.775 cm-1 channel, ECMWF bias is about -1.7 K, whereas NCEP is about -3.6 K. At this level, there is not much observed data used to constrain the model. One can conclude that the ECMWF's temperature analysis in the upper stratosphere appears to be more accurate than NCEP's. As mentioned above, differences in the stratosphere are likely due to differences in model height and the data assimilated. However in the troposphere, any differences must be due to other causes. The differences for the water vapor channels, shown in Fig. 10, are particularly interesting and warrant further investigation.

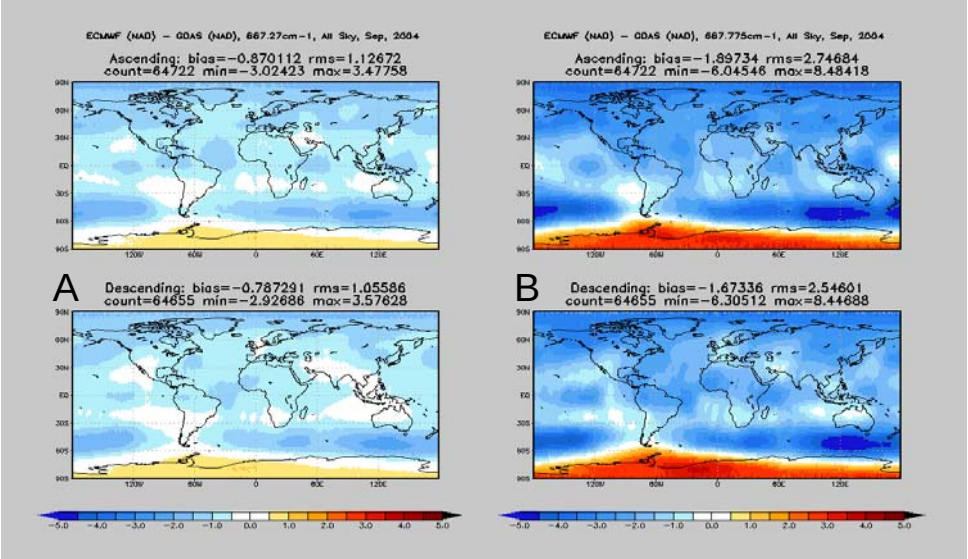

Figure 9: ECMWF minus GDAS simulated brightness temperatures for A: 667.27 cm-1 (15 mb) and B: 667.775 cm-1 (1.5 mb)

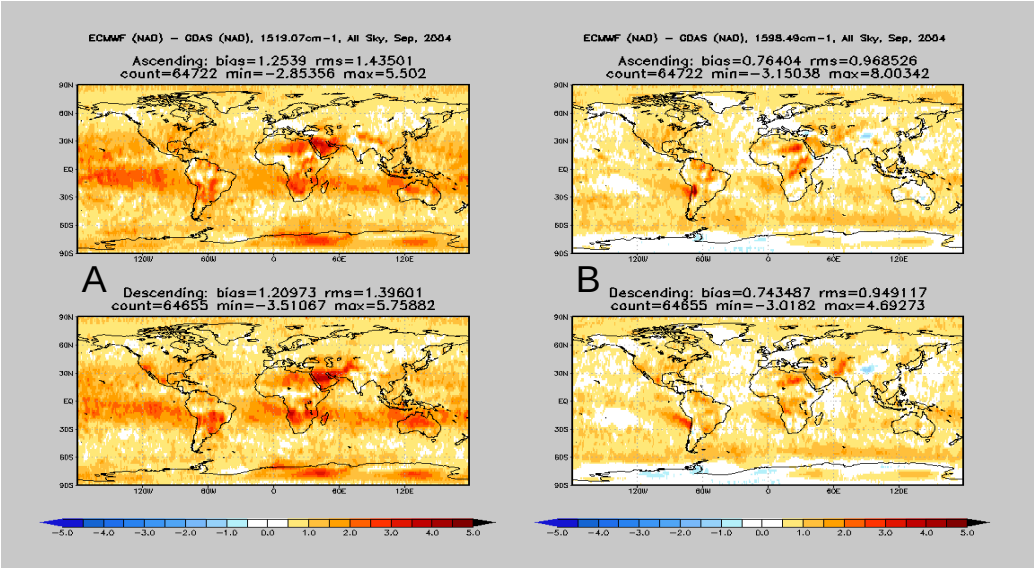

Figure 10: ECMWF minus GDAS simulated brightness temperatures for A: 1519.07 cm-1 (315 mb) and B: 1598.45 cm-1 (490 mb)

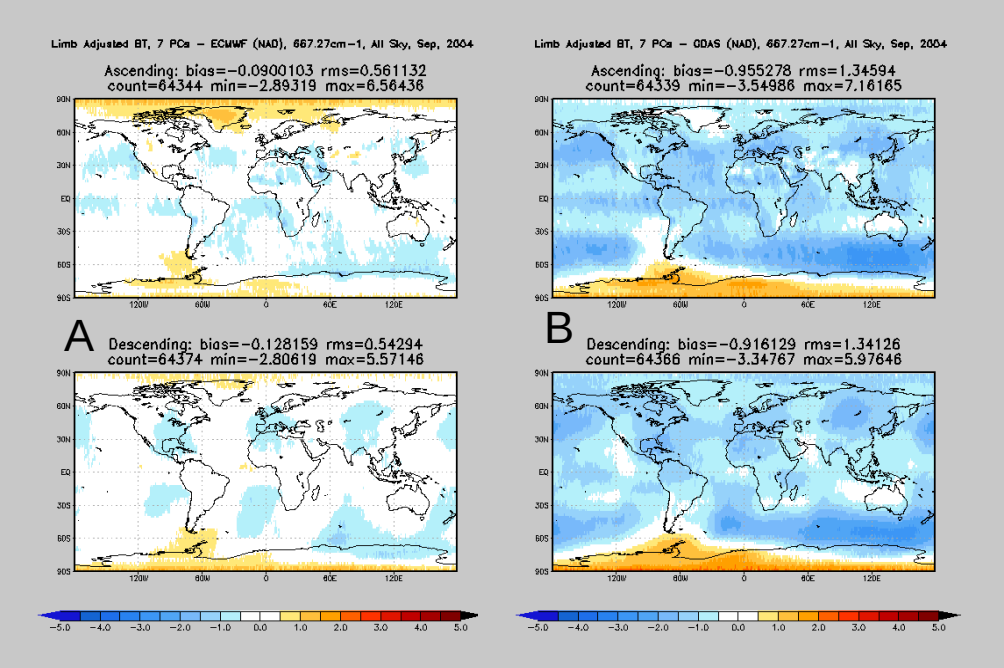

Figure 11: Difference between limb adjusted AIRS and simulated ECMWF brightness temperatures (A) and with NCEP (B) for 667.27 cm-1 (15 mb)

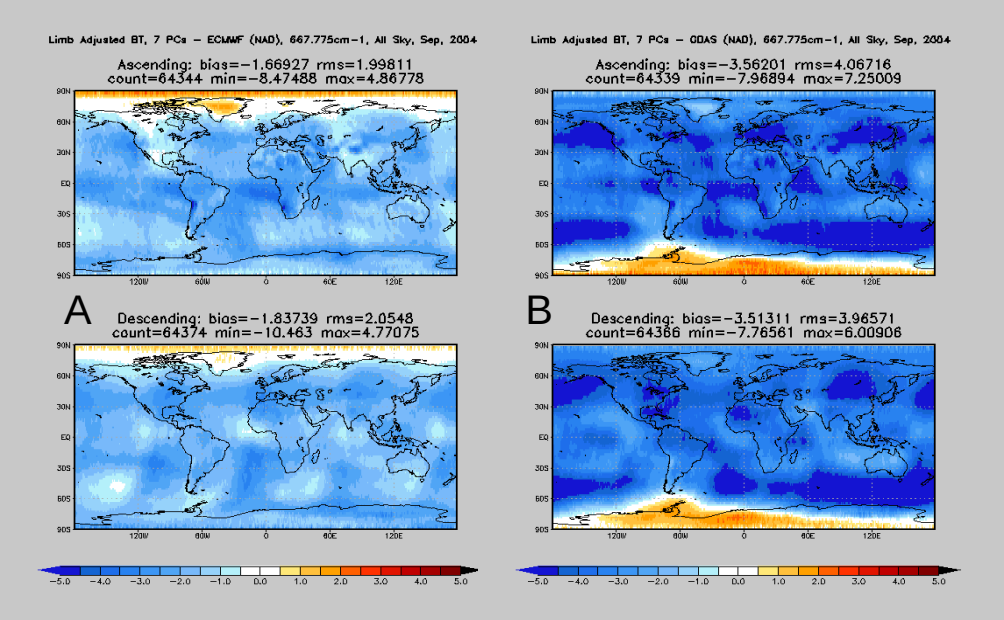

Figure 12: Difference between limb adjusted AIRS and simulated brightness temperatures (A) ECMWF and (B) NCEP for 667.775 cm-1 (1.5 mb)

Figure 13 shows the difference between the ECMWF and NCEP total precipitable water vapor fields and their mean for September 2003 and 2004. Both difference fields show a moist bias of about 1 mm in the NCEP field with respect to the ECMWF field.

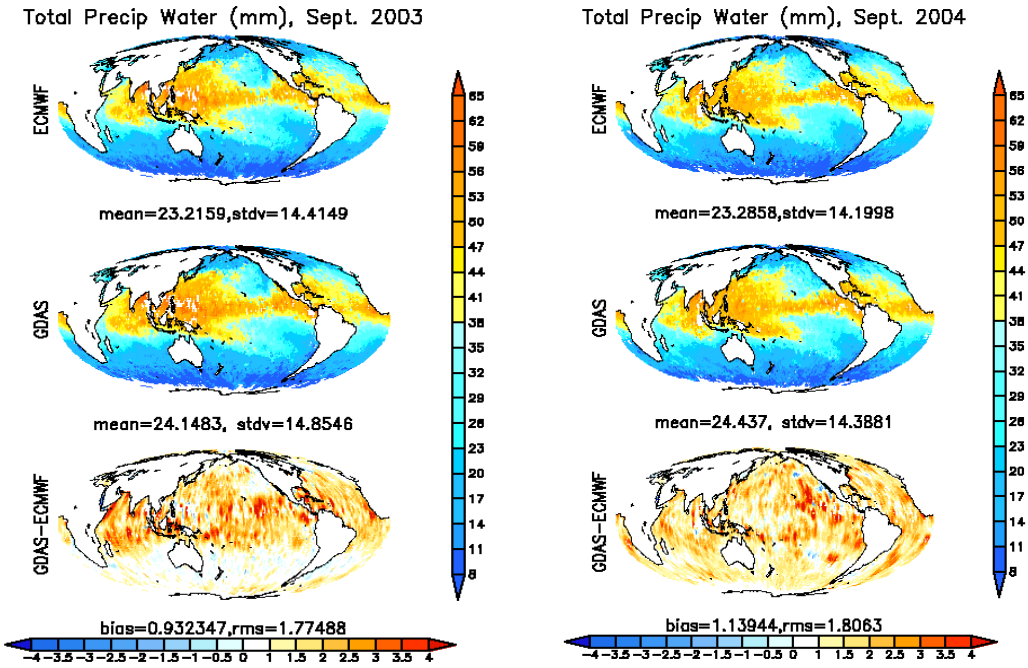

Figure 13: Comparisons of ECMWF and GDAS Total Precipitable Water for September 2003 and 2004.

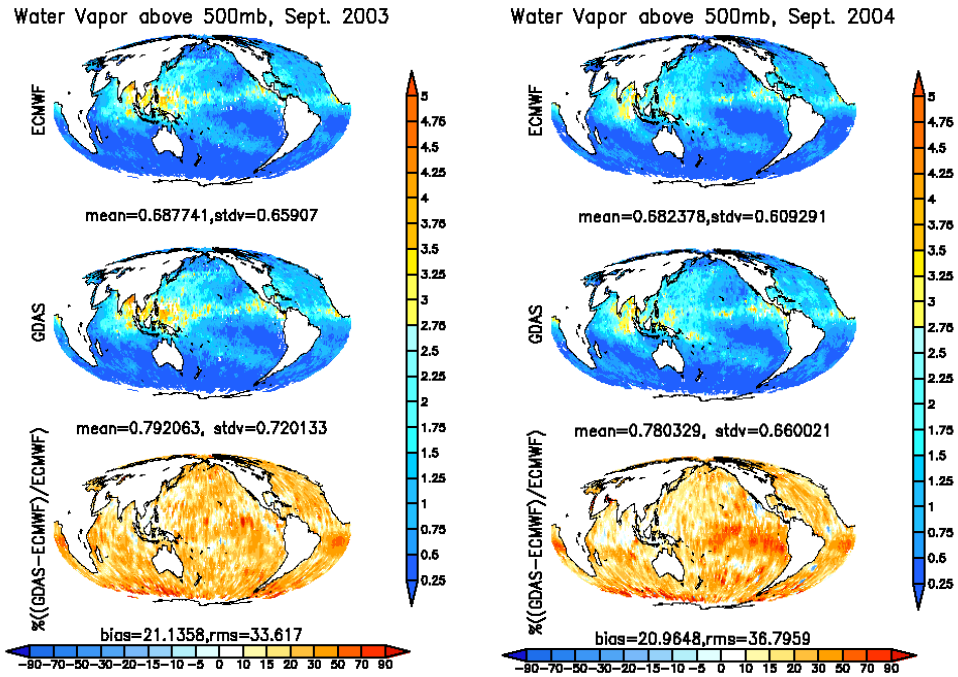

Figure 14: Comparisons of ECMWF and GDAS above 500 mb precipitable water for September 2003 and 2004

Figure 14 shows the difference between the ECMWF and NCEP total precipitable water vapor fields above 500 mb and their mean for September 2003 and 2004. Both difference fields show a moist bias of about 20%

in the NCEP field. To determine which model analysis is most accurate with respect to water vapor, brightness temperatures are simulated using NCEP and ECMWF temperature and moisture analysis fields. Because the clear detection algorithm and the radiative transfer model are more accurate over ocean, and surface emissivity is better known, the brightness temperatures simulations are restricted to ocean areas.

Figure 15 shows the ECMWF and NCEP biases (computed minus measured) for the entire AIRS spectral range for September 2003 and 2004. The clear detection algorithm threshold based on SST [Goldberg et al., 2003] was relaxed to allow for a larger population of clear cases, about 35% instead of just 5%. As a result, there is a positive bias of about 1 K for the window channels (800 -1000 cm^{-1}, 1070 – 1250 cm^{-1} and 2400 – 2650 cm^{-1}) due to low cloud contamination. However, for mid to upper tropospheric water vapor channels (1450 – 1600 cm^{-1}), the relaxed test does not introduce appreciable cloud contamination. Figure 15, shows that the largest ECMWF bias in the water vapor region is about - 0.7 K, whereas for NCEP it is about -2.4 K.

From Fig. 2, it can be inferred that a differences of the two biases, which is 1.7 K, results in a change in water vapor of about 20%, which is approximately the same value show in Fig. 5.14. The standard deviations of the computed minus measured differences are plotted in Fig. 16, which shows a lower standard deviation with respect to ECMWF. ECWMF started to assimilate AIRS radiances operationally in October, 2003, whereas NCEP operational use of AIRS began in May, 2005. Inspection of Figs. 15 and 16 suggests a small impact of AIRS data in the ECMWF analysis, because the difference between September 2003 and 2004 appears to be small. However these figures represent a global average, so a closer examination is needed for the two water vapor channels shown in Fig. 10.

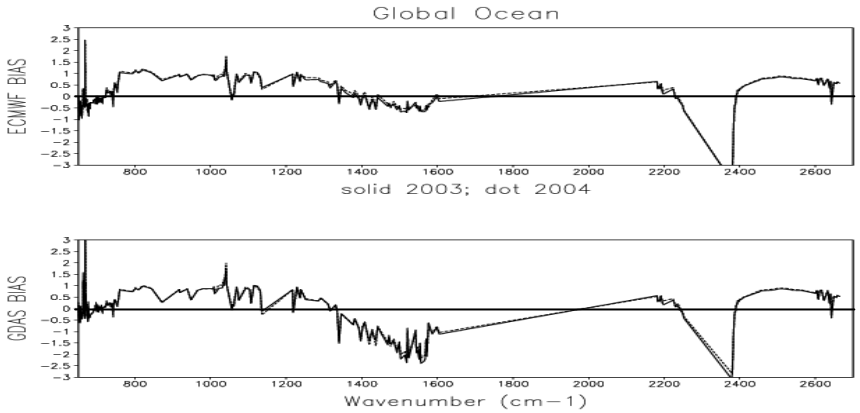

Figure 15: Bias of AIRS measured minus computed from ECMWF (upper) and NCEP GDAS (lower) for September 2003 and 2004

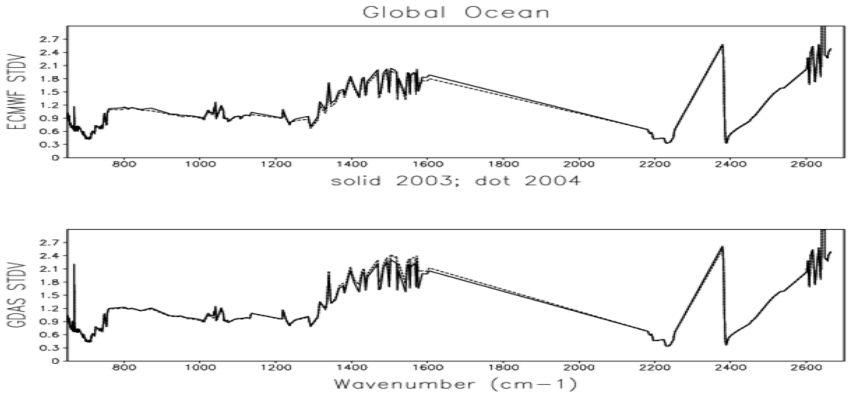

Figure 16: Standard deviation of AIRS measured minus computed from ECMWF (upper) and NCEP GDAS (lower) for September 2003 and 2004

Shown in Fig. 17 are the observed AIRS minus simulated ECWMF brightness temperatures for the 1519.07 cm^{-1} (315 mb) upper tropospheric water vapor channel, for September 2003, 2004 and 2005. Fig. 18 shows the comparable figure using the NCEP analysis. Fig. 17 shows relatively smaller biases for all three periods, demonstrating that ECMWF analysis water vapor fields were relatively accurate even before AIRS was assimilated. The rms was reduced by about 0.3 K. Note that the absence of locally large deviations after 2003. In Fig. 18, there was a very large reduction in the bias (September 2005) after AIRS was used operationally by NCEP. The bias was reduced by more than 1 K and the rms was reduced by nearly 1 K. Figs. 19 and 20 show the results for the mid-tropospheric 1598.45 cm^{-1} (490 mb) channel.

For the mid tropospheric channel, the ECMWF bias is only about 0.1 K. The bias does not change much over the three different years. However there is a reduction in the rms, from approximately 1.5 K to 1.15 K, after AIRS is assimilated operationally. In the case of NCEP, the bias is larger, about 0.9 K, however it does decrease to about 0.6 K in 2005, after AIRS is assimilated operationally by NCEP. There is a small reduction in the rms. However a large bias in excess of 4 K is found over the eastern Pacific just south of the equator. This is very interesting because the feature is nonexistent in ECWMF, and the cause remains unknown. In summary, the ECMWF analyses are shown to be more consistent with the AIRS radiance climatology

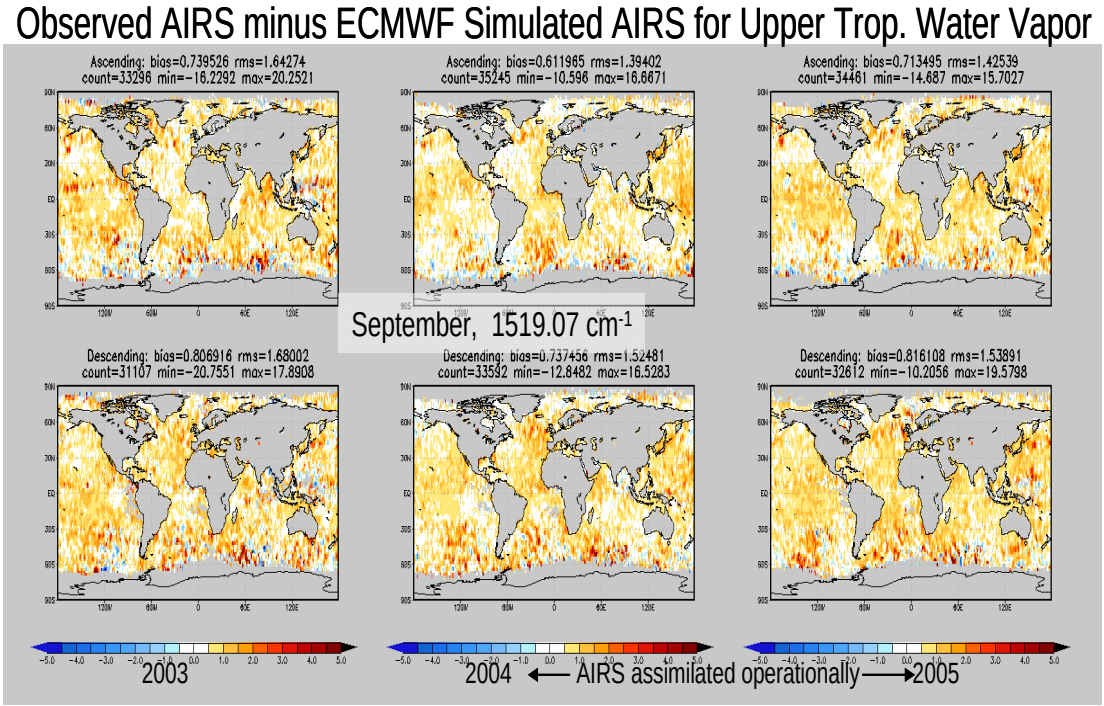

Figure 17: Observed AIRS minus ECMWF simulated AIRS for upper tropospheric water vapor channel at 1519.07 cm-1 wavenumber.

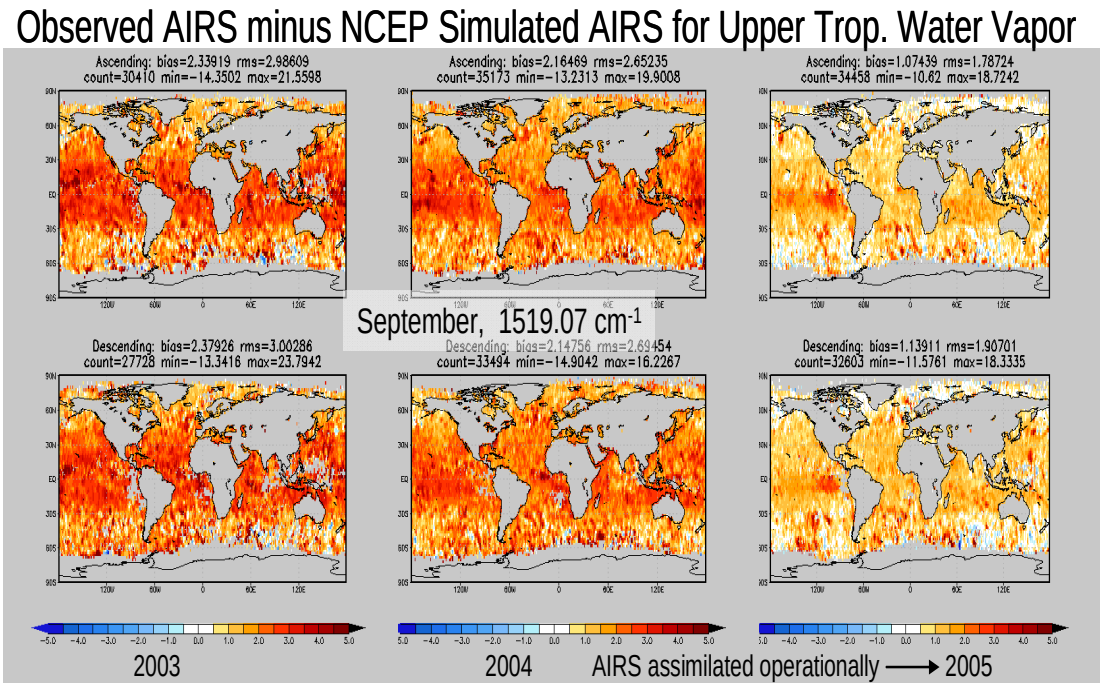

Figure 18: Observed AIRS minus NCEP simulated AIRS for upper tropospheric water vapor channel at 1519.07 cm-1 wavenumber.

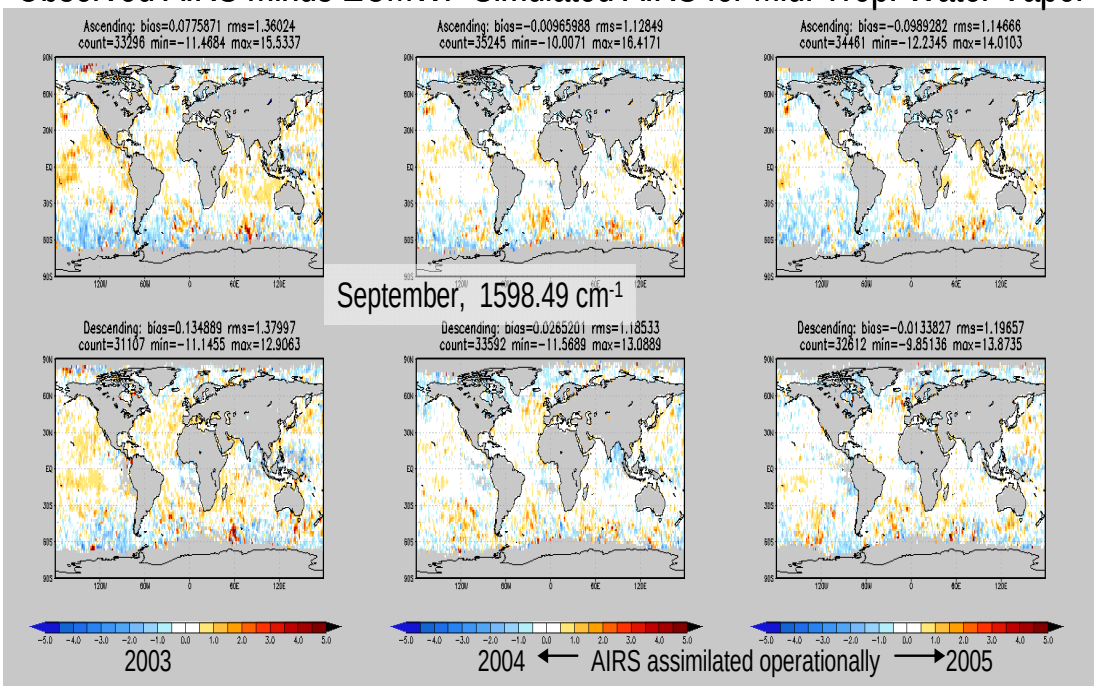

Figure 19: Observed AIRS minus ECMWF simulated AIRS for middle tropospheric water vapor channel at 1598.45 cm^{-1} wavenumber.

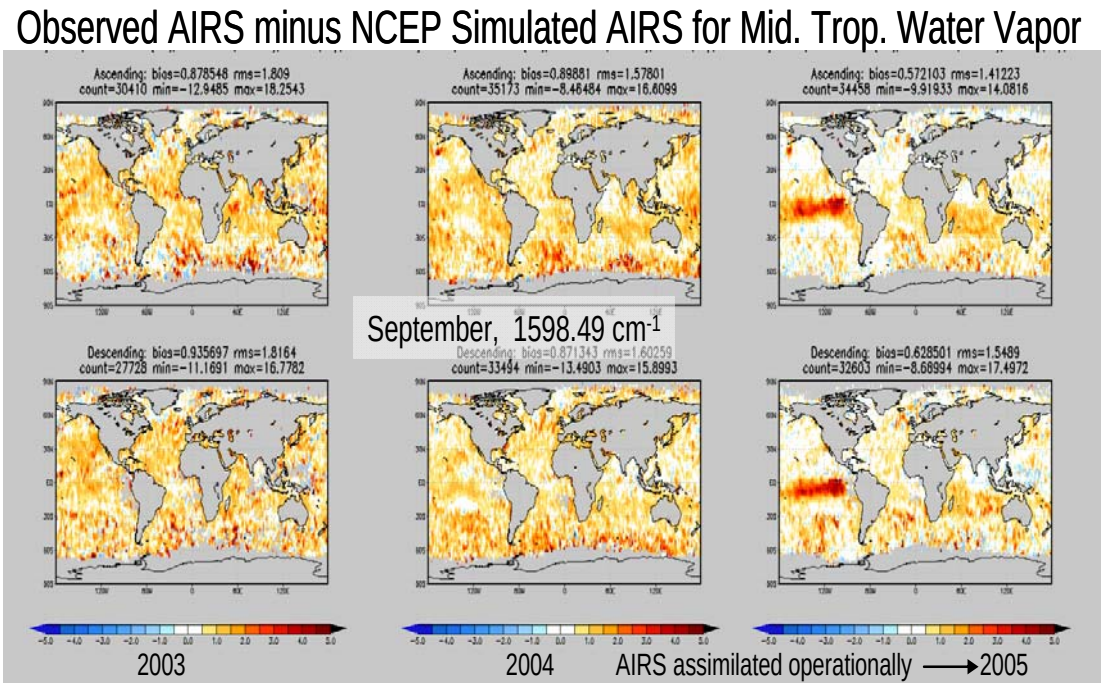

Figure 20: Observed AIRS minus NCEP simulated AIRS for middle tropospheric water vapor channel at 1598.49 cm^{-1} wavenumber.

5. Summary of NCEP and ECMWF Analysis Validation

The AIRS radiance climatology has been demonstrated to have significant value in validating NWP model analyses. Based on the above results, one can conclude that, for the period of 2003 to 2005, ECMWF's analyses appear to be more accurate than NCEP's and in excellent agreement with AIRS observations, except for the upper stratosphere. Unfortunately, in 2006 the AIRS radiance climatology detected degradation in the ECMWF water vapor analysis, underscoring the importance of the AIRS data for ongoing validation. After a number of operational upgrades of the ECMWF data assimilation system including revisions to the cloud scheme, the implicit computation of convective transports, and variational radiance bias adjustments, the bias in the upper tropospheric water vapor channel for September 2006, shown in Fig. 21, increased significantly to 1.55 K from 0.71 K in September 2005 and is now larger than that of NCEP. Fig. 22 shows the biases for the lower tropospheric water channel for September 2006. The bias has increased to 0.43 K (September 2006) from -0.10 K September (2005); however the bias for this channel remains lower than the NCEP bias. Table 1 is the tabulation of the biases given in previous figures Notice how the precipitable water above 500 mb for ECMWF (row d) in 2006 departs significantly from the mean values for 2003 through 2006. The difference between NCEP and ECMWF precipitable water above 500 mb (row f), shown is only a fraction of a percent in 2006; in 2003 and 2004 it was about 21%, decreasing to 11.45% in 2005. Further inspection of Table 1 shows a strong relationship between rows m and f. Row m is the sum of rows i (the difference of the NCEP and ECMWF bias for 1519 cm^{-1}) and l (the difference of the NCEP and ECMWF bias for 1598 cm^{-1}). This should be expected since both channels together are more sensitive to the water vapor above 500 mb, as opposed to the total precipitable water. The relationship between the numerical values in rows f and m can be approximated very accurately with a polynomial expression ($f = 2.38 – 9.96m – 0.92m^2$) with Pearson correlation squared (r^2) of 0.9992.

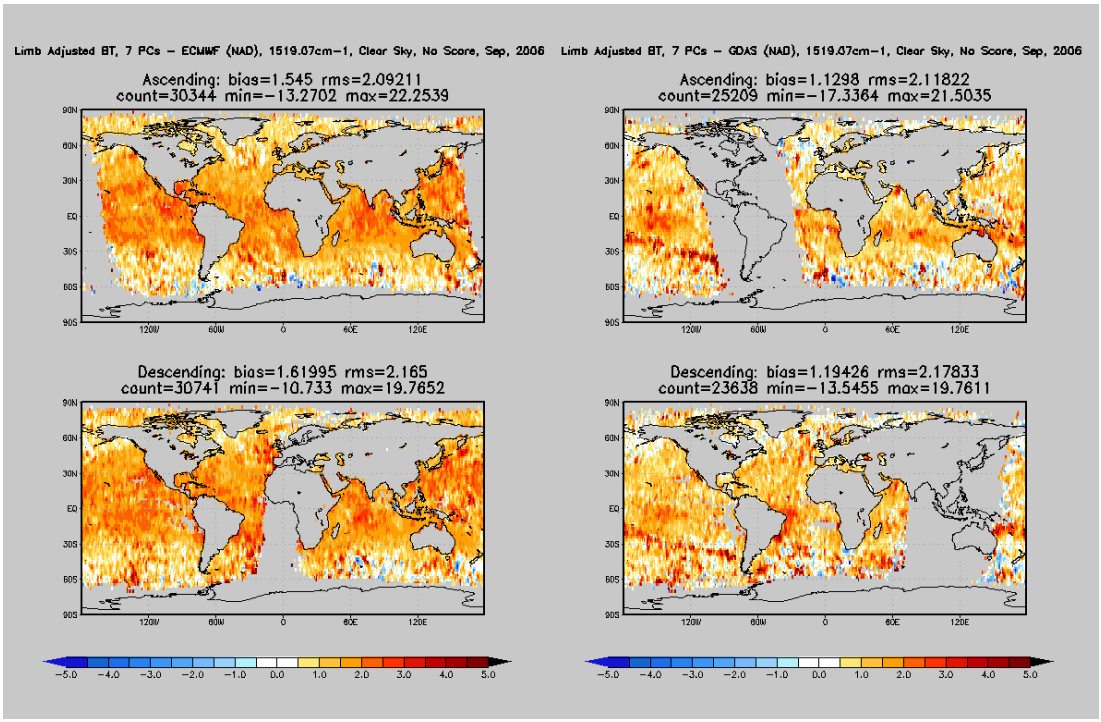

Figure 21: Observed AIRS minus ECMWF simulated AIRS (left panel) and observed AIRS minus NCEP simulated AIRS (right panel) for upper tropospheric water vapor channel at 1519.07 cm^{-1} wavenumber for September 2006.

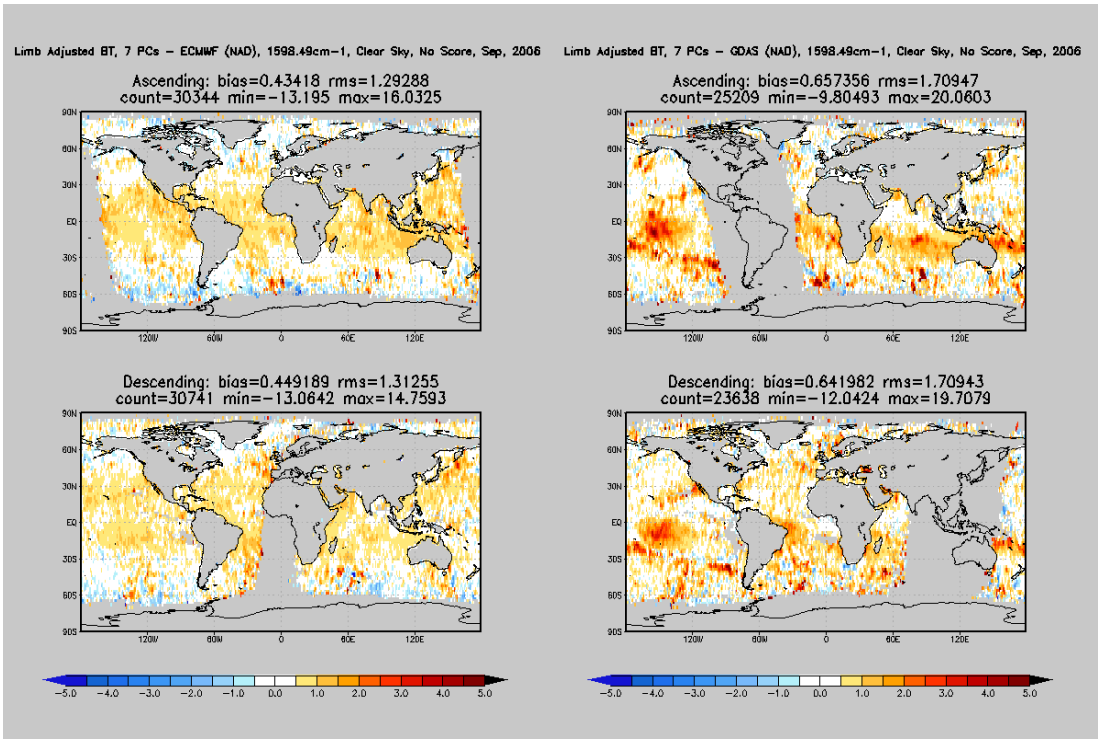

Figure 22: Observed AIRS minus ECMWF simulated AIRS (left panel) and observed AIRS minus NCEP simulated AIRS (right panel) for lower tropospheric water vapor channel at 1598.49 cm^{-1} wavenumber for September 2006.

Table 1 Summary of Bias

		2003	2004	2005	2006
a	ECMWF TPW	23.22 mm	23.29	22.70	22.34
b	NCEP TPW	24.15 mm	24.44	24.02	24.01
c	NCEP - ECMWF	0.93 mm	1.14	1.32	1.67
d	ECMWF PW above 500mb	0.69 mm	0.68	0.68	0.75
e	NCEP PW above 500 mb	0.79 mm	0.78	0.75	0.75
f	NCEP - ECMWF	21.14%	20.96%	11.45%	0.37%
g	ECMWF 1519cm^{-1}	0.73 K	0.61	0.71	1.55
h	NCEP 1519cm^{-1}	2.34 K	2.16	1.06	1.13
i	NCEP – ECMWF*	-1.61 K	-1.55	-0.35	0.42
j	ECWMF 1598cm^{-1}	0.10 K	-0.01	-0.10	0.43
k	NCEP 1598cm^{-1}	0.86 K	0.90	0.56	0.65
l	NCEP – ECMWF*	-0.76 K	-0.91	-0.66	-0.22
m	SUM OF DIFF*	-2.37 K	-2.46	-1.01	0.20

6. Concluding Remarks

The operational IASI on the MeTOP satellite series and the future operational CrIS on the NPOESS satellite series will provide continuous observations of high spectral resolution infrared radiances well into the 2020s. Both AIRS and IASI are now in orbit, and intercomparisons of both sensors have generally shown brightness temperature differences between the two sensors of less than 0.1 K. Most importantly, the recently computed trend of the differences is less than .01 K per year, which means both sensors have the stability and the fidelity to accurately detect long term trends of at least a few tenths of a degree K per decade. Follow-on missions will continue this type of measurement well into this century. Long-term stability of infrared sensors require internal blackbody targets with very high emissivities approaching unity (generally the requirement is > 0.9995). Both AIRS and IASI meet these requirements; however there is no internal monitoring to determine whether the high blackbody emissivity is maintained in orbit. This is why continuous intercomparisons between AIRS and IASI, and later CrIS is needed to demonstrate long term stability. NASA is considering a new mission called Climate Absolute Radiance and Refractivity Observatory (CLARREO), which measures outgoing radiances in the far, near and thermal infrared with high spectral resolution, high stability and internal monitoring. The CLARREO instrument will have a relatively large field of view (~ 100 km), and only nadir. It will have difficulty providing sufficient data sampling for examining regional trends and variability, however it can be used as a benchmark measurement to verify, and anchor if necessary, the stability of the multiple applications (i.e. weather and climate) of operational high spectral resolution infrared sounders such as AIRS, IASI, and CrIS.

7. References

Aumann, H.H., M.T. Chahine, C. Gautier, M.D. Goldberg, E. Kalnay, L.M. McMillin, H. Revercomb, P.W. Rosenkranz, W.L. Smith, D.H. Staelin, L.L. Strow and J. Susskind 2003: AIRS/AMSU/HSB on the Aqua mission: design, science objectives, data products, and processing systems. *IEEE Trans. Geosci. Remote Sens*. **41**, 253-264.

Aumann, H.H., S. Broberg, D. Elliott, S. Gaiser and D. Gregorich 2006: Three years of Atmospheric Infrared Sounder radiometric calibration validation using sea surface temperature. *J. Geophys. Res*. **111**

Goldberg, M. D., D. S., Crosby, and L. Zhou, 2001: The limb adjustment of AMSU A observations: methodology and validation. *J. Appl. Meteor*., **40**, 70-83.

Goldberg, M.D., Y. Qu, L.M. McMillin, W.W. Wolf, L. Zhou and M. Divakarla 2003: AIRS near-real-time products and algorithms in support of operational weather prediction. IEEE Trans. *Geosci. Remote Sens*., **41**, 379-389.

Goldberg, M.D. 2009: The Generation and Applications of a Spectrally Resolved Infrared Radiance Climatology derived from the Atmospheric Infrared Sounder, PhD Dissertation, University of Maryland, 118 pgs.

Schiermeier, Q., Arctic trends scrutinized as chilly winter destroys ozone, *Nature* **435**, 6 (5 May 2005) *Nature*, **449**, 382-383 (2007)

Strow, L.L., S.E. Hannon, S. DeSouza-Machado, H.E. Motteler and D.C. Tobin, 2003: An overview of the AIRS radiative transfer model. *IEEE Trans. Geosci. Remote Sens*., **41**, 303-313

Tobin, D.C., H.E. Revercomb, R.O. Knuteson, F.A. Best, W.L. Smith, N.N. Ciganovich, R.G. Dedecker, S. Dutcher, S.D, Ellington, R.K. Garcia, H.B. Howell, D.D LaPorte, S.A. Mango, T.S. Pagano, J.K Taylor, P. Van Delst, K.H. Vinson and M.W. Werner, 2006: Radiometric and spectral validation of Atmospheric Infrared Sounder observations with the aircraft-based Scanning High-Resolution Interferometer Sounder. *J. Geophys. Res*., **111** D09S02 doi:10.1029/2005JD006094, 14 pgs.

Tobin, D., et al. (2008), Evaluation of IASI and AIRS spectral radiances using Simultaneous Nadir Overpasses, paper presented at 16th International TOVS Study Conferences, Angra dos Reis, Brazil.

Wang L., C. Cao, and M. Goldberg, 2009a: Inter-calibration of GOES-11 and GOES-12 water vapor channels with MetOp/IASI hyperspectral measurements. *J. Atmos. Oceanic Technol.* (Accepted upon revision).

Wang, L., X. Wu, Y. Li, M. Goldberg, S.-H. Sohn, and C. Cao, 2009b: Comparison of AIRS and IASI radiances using GOES imagers as transfer radiometers toward climate data records. *J. Appl. Meteor. Climate* (submitted).

Acknowledgements and Disclaimers

The contents are solely the opinions of the authors and do not constitute a statement of policy, decision, or position on behalf of NOAA or the United States government. The authors gratefully acknowledge the support of the NASA EOS program, the AIRS science team and the NPOESS Integrated Program Office